pubs.acs.org/Biomac

Article

Strengthening and Toughening of Protein-Based Thermosets via Intermolecular Self-Assembly

Yiping Cao and Bradley D. Olsen*

Cite This: *Biomacromolecules* 2022, 23, 3286−3295

Read Online

ACCESS | Metrics & More | Article Recommendations | Supporting Information

ABSTRACT: As proteins are abundant polymers in biomass sources such as agricultural feedstocks and byproducts, leveraging them to develop alternatives to synthetic polymers is of great interest. However, the mechanical performance of protein materials is not suitable for most target applications. Constructing copolymers with proteins as hard domains and rubbery polymers as soft domains has been shown to be a promising strategy for improving mechanical properties. Herein, it is demonstrated that toughening and strengthening of protein copolymers can be advanced further by thermal treatment, leading to mechanical enhancements that generalize across a variety of different protein feedstocks, including whey, serum, soy, and pea proteins. The thermal treatment induces a rearrangement of protein structure, leading to the formation of intermolecular β-sheets. The ordered intermolecular structures in the hard domains of thermosets greatly improve their mechanical properties, providing simultaneous increases in strength, toughness, and modulus, with little sacrifice in fracture strain. Analogous to crystalline structures, the formation of intermolecular β-sheet structures also leads to reduced hygroscopicity. This is a valuable contribution, as practical applications of natural polymer-based plastics are frequently hindered by the materials' humidity sensitivity. Therefore, this work demonstrates a simple yet versatile strategy to improve the materials' performance from a wide range of protein feedstocks, as well as signifies the implications of protein structural assembly in materials design.

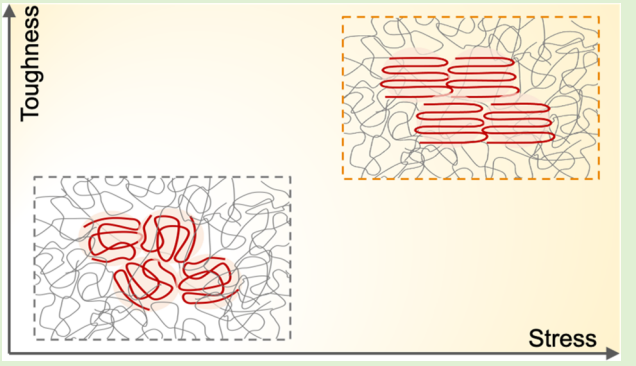

INTRODUCTION

Replacing conventional plastics with biomass-based ones is an attractive strategy to address the current plastics crisis, as bioplastics reduce fossil fuel consumption and are often degradable or compostable.[1−4] A great deal of work is focused on sugar-based replacements, including synthetic biopolymers such as poly(lactic acid) and poly(butylene succinate) or natural biopolymers such as starch and cellulose.[1−4] However, a large number of materials such as polyamides and polyurethanes that need to be replaced are based on amide bonds,[5−7] indicating the importance of nitrogen-containing feedstocks. As the most abundant nitrogen-containing feedstocks and a macromolecule capable of generating hydrogen bonds and crystalline structures similar to polyurethanes,[8−10] proteins represent attractive materials for the development of plastic replacements. Several studies have shown that the concept of fabricating large-scale materials from protein feedstocks holds great economic promise, suggesting the key science and technology gap now is the development of protein materials with desired performance.[11−13]

Pure protein materials are typically stiff and brittle due to the extensive forces through hydrogen bonds, electrostatic interactions, hydrophobic interactions, and disulfide bonds.[14] Plasticizers, such as glycerol and ethylene glycol, are often used to make protein materials easier to process and to provide extensibility and flexibility.[1,14−16] Surfactants can lower the melting point by disrupting molecular interactions, allowing proteins to be liquefied and processed in the absence of solvents.[17,18] However, plasticizers and surfactants sacrifice stiffness and strength and tend to absorb moisture, causing further reduction in mechanical properties.[1,14−18] Blending of proteins with soft polymers (polymers with low glass transition temperature T_g) can achieve extensibility and toughness without such dramatic sacrifices in strength and stiffness. Examples include proteins added to rubbers that can aggregate and form reinforcing networks[19] and proteins or protein fibrils blended with poly(vinyl alcohol).[20] Given that polymer blends frequently suffer from compatibility issues, copolymers would be promising candidates for the development of high-performance and stable thermosets.[21]

Current protein copolymers designed for excellent mechanical properties are mainly derived from well-defined pepti-

Received: March 25, 2022
Revised: June 8, 2022
Published: July 14, 2022

https://doi.org/10.1021/acs.biomac.2c00372
Biomacromolecules 2022, 23, 3286−3295

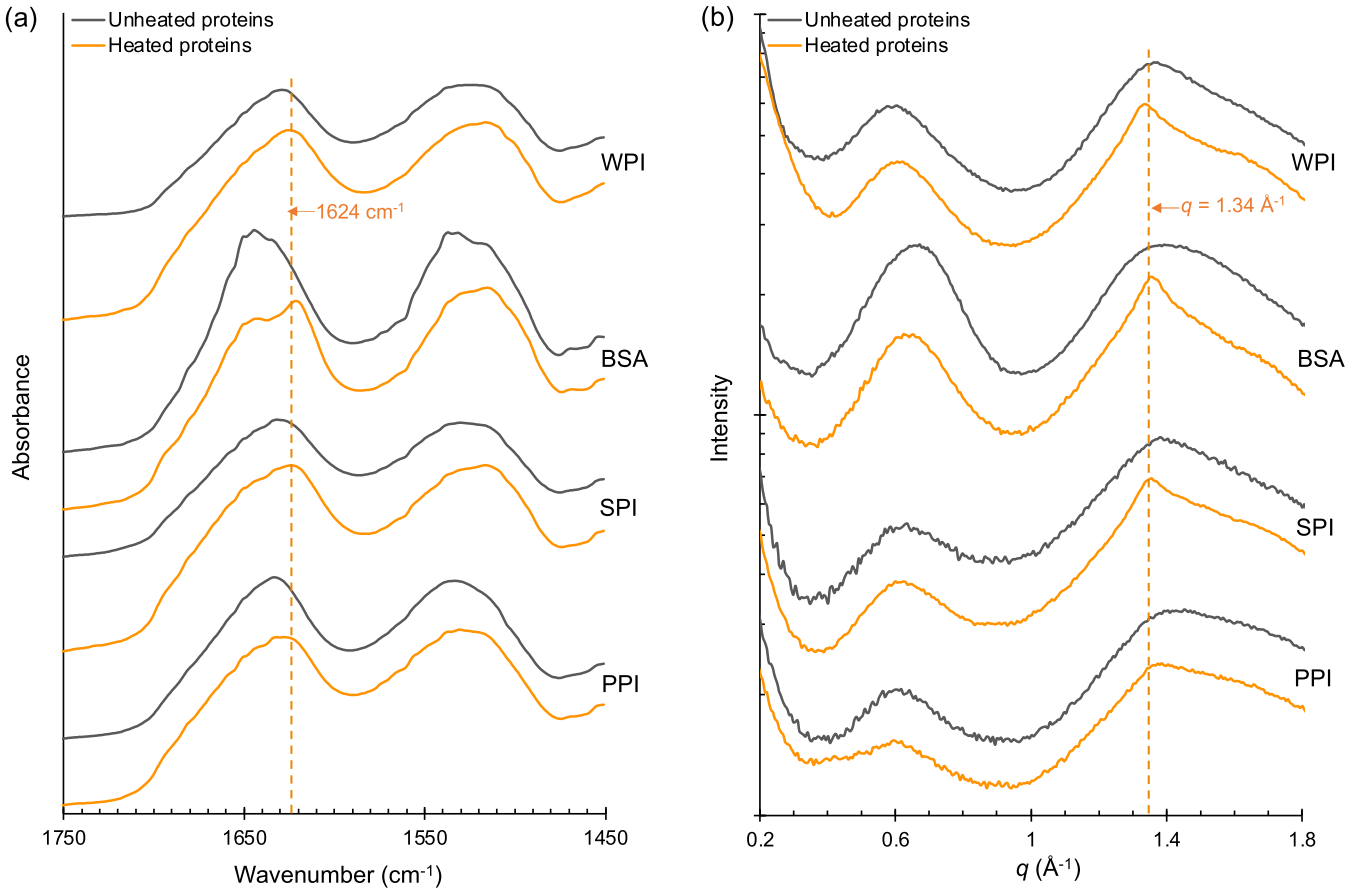

Figure 1. Structural characterization of unheated and heated proteins. (a) FTIR spectra. The dashed line at 1624 cm^{-1} features the intermolecular β-sheet structures. (b) WAXS spectra. A sharp peak appears for heated proteins at $q = 1.34$ $Å^{-1}$, namely $d = 2\pi/q = 4.69$ Å, which is the distance between adjacent β-strands in the ordered β-sheets. Whey protein isolate (WPI), bovine serum albumin (BSA), soy protein isolate (SPI), and pea protein isolate (PPI) were measured. Heat treatment was performed at 100 °C and pH 7.

des,[22−25] such as copolymers composed of silk-inspired peptide sequences and poly(ethylene oxide)[25] or copolymers composed of amyloidogenic peptide sequences and flexible linkers,[23] where the peptides form ordered β-sheet structures to provide stiffness and poly(ethylene oxide)/flexible linkers provide extensibility. Although peptides with well-defined sequences offer opportunities to design high-performance copolymers, they are relatively costly and difficult to produce on a large scale.[26] An important solution to address this limitation lies in using crude agricultural proteins as feedstock. Our group has shown that copolymers can be synthesized from crude proteins by acrylating proteins and then copolymerizing them with acrylate monomers.[8−10] The resulting copolymers, although outperforming either polymer blends or single polymer networks in terms of strength and toughness, cannot achieve the mechanical properties of many synthetic polymer systems. Therefore, the efficient development of high-performance copolymers from crude proteins remains a challenge.

Inspired by the cooking-induced textural hardening of regular and plant-based meat (typical protein materials), this study investigates the effect of thermal treatment on the properties of protein copolymers. Thermosets dried from protein−polyacrylate copolymer gels were chosen as the model system because of their great potential as partially renewable alternatives to engineering plastics such as polyurethanes, where proteins act as hard domains and low-T_g poly(hydroxypropyl acrylate) (PHPA) as soft domains. Protein structural changes induced by heat treatment were investigated to understand how such structural changes affect the material properties. Whey protein isolate (WPI), bovine serum albumin (BSA), soy protein isolate (SPI), and pea protein isolate (PPI) were chosen as material feedstocks for their well-characterized structures, renewable origins, and wide availability; for example, WPI and SPI are byproducts of cheese and soybean oil production.[27,28]

EXPERIMENTAL SECTION

Materials. Hydroxypropyl acrylate (HPA), methacrylic anhydride, ammonium persulfate (APS), and basic activated alumina were obtained from Sigma-Aldrich. Tetramethylethylenediamine (TEMED) was purchased from Alfa Aesar. Whey protein isolate (WPI), whey protein concentrate (WPC), whey protein powder (WPP), bovine serum albumin (BSA), soy protein isolate (SPI), and pea protein isolate (PPI) were purchased from Nutricost, Nutricost, Orgain, Sigma-Aldrich, Bulk Supplements, and Naked Nutrition, respectively. The details and the protein content of these six protein samples are given in Table S1.

Preparation of Methacrylated Protein Solutions. As crude protein powders are mainly produced by spray-drying (with severe protein aggregation), they are not completely soluble at neutral pH. To remove insoluble proteins, 10−20 wt % crude protein solution was centrifuged three times at 15 000*g*. Protein concentration in the supernatant was measured by the dry-weight method and adjusted to 10 wt % for WPI and BSA, 6 wt % for SPI, and 3 wt % for PPI. The relatively low concentrations of SPI and PPI used were due to the higher concentrations being too viscous to be uniformly mixed and

https://doi.org/10.1021/acs.biomac.2c00372
Biomacromolecules 2022, 23, 3286−3295

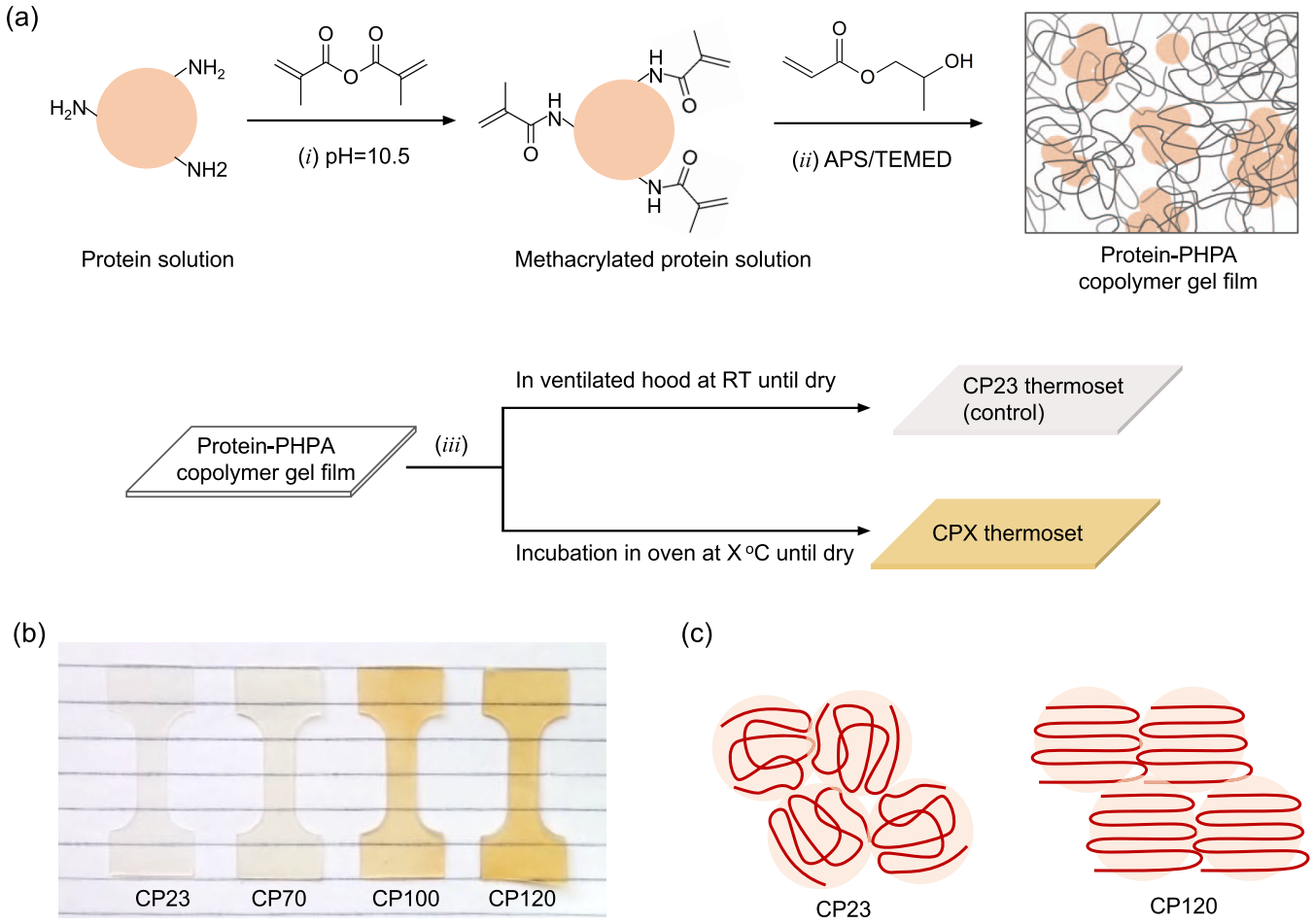

Figure 2. (a) Schematic diagram of the preparation of protein-PHPA copolymer thermosets: (i) reaction of protein amino groups with methacrylic anhydride; (ii) copolymerization of methacrylated proteins with acrylate monomers, with the formation of gel film; and (iii) the copolymer gel films are incubated in an oven at temperature up to 120 °C to induce protein structural rearrangement or in a ventilated hood at room temperature as the control, accompanied by water evaporation yielding thermosets. (b) Photographs of WPI-PHPA copolymer thermosets. (c) Structural illustration of protein domains in copolymers, the formation of ordered intermolecular β-sheet structures for thermally treated copolymers. CPX refers to the thermoset prepared by incubating copolymer (CP) gel at temperature X °C.

copolymerized. For the preparation of WPC and WPP solutions (dispersions), the centrifugation step was not applied. Namely, 10 wt % WPC and 10 wt % WPP were prepared by directly mixing 1 mass equivalent of protein powder with 9 mass equivalents of MQ water and stirring overnight.

Methacrylated proteins were prepared using the anhydride−amine reaction, in which polymerizable methacrylate groups were attached to protein molecules. After adjusting the pH of the above protein solution to 10.5 using sodium hydroxide, methacrylic anhydride was added while stirring to an anhydride-to-protein mole ratio of 3 calculated using the molecular weight of β-lactoglobulin (18.4 kDa) for all proteins. The reaction was carried out overnight under ambient conditions, and the product was used for subsequent copolymerization without purification.

Preparation of Unheated and Heated Proteins. Unheated and heated protein samples (pure protein systems) were prepared from the methacrylated protein solution. Typically, 1 mL of protein solution with pH adjusted to 7 was pipetted into ϕ = 15 mm Teflon disks and placed in a ventilated hood at room temperature (referred to as unheated proteins) or in an oven at 100 °C (referred to as heated proteins) until dry. This condition was applied to keep consistency with the thermoset preparation process. Unheated and heated proteins were used for FTIR and WAXS measurements (Figure 1) to illustrate the effect of heat treatment on protein structural changes in pure protein systems.

Preparation of Protein−Polyacrylate Copolymer Gels and Thermosets. Protein−polyacrylate copolymer gels were prepared by free-radical copolymerization of methacrylated proteins and acrylate monomers. Prior to copolymerization, hydroxypropyl acrylate (HPA) was passed through basic alumina to remove the inhibitor, and the methacrylated protein solution was adjusted to pH 7 to minimize protein hydrolysis during the heat treatment. In a typical process of preparing WPI-PHPA gels, 30 g of 10 wt % methacrylated WPI solution was mixed with 9 g of HPA monomer, followed by the introduction of 500 μL of 100 mg/mL ammonium persulfate (as the initiator) and 10 μL of TEMED (as the catalyst), corresponding to the initiator/catalyst to monomer mole ratios of ∼1:300 and 1:1000. The mixture was immediately transferred between two parallel glass plates with a 1 mm spacer, and the reaction was performed overnight under ambient conditions to form gelled samples. For copolymer gels from other proteins, the amount of HPA was adjusted accordingly with the initial protein concentration to achieve the targeted protein-to-acylate mass ratio.

Thermosets were prepared by incubating protein−polyacrylate copolymer gels at different temperatures. The gel samples were peeled from the glass plates and incubated in an oven to trigger protein self-assembly. The incubation times corresponding to temperatures of 70, 100, and 120 °C are 12, 5, and 3 h, respectively. During this period, water evaporation leads to the formation of thermosets, referred to as CP70, CP100, and CP120, respectively. The thermoset prepared by drying the copolymer gels in the ventilated hood at room temperature was used as the control, referred to as CP23. Prior to characterization,

https://doi.org/10.1021/acs.biomac.2c00372
Biomacromolecules 2022, 23, 3286−3295

thermosets were equilibrated at the corresponding relative humidity (RH) and 23 °C for 3 days.

Fourier Transform Infrared Spectroscopy (FTIR). Protein secondary structures in copolymers and pure proteins were investigated using a Bruker ALPHA II FTIR spectrometer equipped with a diamond crystal attenuated total reflection (ATR). FTIR absorption spectra in ATR mode were recorded at room temperature over the wavenumber range of 4000−400 cm^{-1} with 64 scans and a resolution of 4 cm^{-1}. Each sample was subjected to at least three measurements, and a representative curve was reported.

Tensile Tests. The tensile test was performed according to the method developed in ref 8. Specimens used for tensile tests were cut with an ASTM D1708 tensile die (Pioneer-Dietecs), and their thickness was measured by a spiral micrometer. Uniaxial tensile tests were performed on a Zwick Z0.5 machine equipped with 500 N loading cells under laboratory environmental conditions. A constant linear deformation rate of 100% strain/min was applied. The stress−strain curves were obtained by dividing the measured force by the initial cross-sectional area and dividing the measured displacement by the initial clamp distance. At least four specimens were tested for each material, and the mean and deviation were reported.

Moisture Content Measurement. The moisture content of the thermosets was determined by comparing their weights before and after drying. Approximately 80−120 mg thermosets that had been equilibrated for 3 days at the corresponding relative humidity were placed in aluminum micro weighing dishes (VWR International) and dried at ∼120 °C until the weight became stable. The weights of the thermosets before (m_w) and after (m_d) drying were measured with an accuracy of 0.01 mg balance. The moisture content was obtained as $(m_w - m_d)/m_w \times 100\%$. Each sample was measured three times, and the mean and deviation were reported.

Wide-Angle X-Ray Scattering (WAXS). WAXS experiments were performed using a Rigaku 002 microfocus X-ray source with Cu Kα1 radiation (λ = 0.154 nm). The freestanding samples were placed in an evacuated chamber at 0.08 mbar. The scattered intensity was collected by the detector Pilatus3 R 300K with an active area of 83.8 × 106.5 mm^2 and a pixel size of 172 × 172 μm^2. The sample−detector distance was set to 109.1 mm, and the acquisition time was 180 s. The obtained 2D diffraction images were background-corrected, azimuthally averaged, and plotted as 1D scattering profiles using SAXSGUI software.

Statistical Analysis. Statistical analysis was performed on Online Statistical Software Stats.Blue (https://stats.blue). Asterisks identify data sets that are statistically ($p < 0.05$) different from the control experiment.

RESULTS AND DISCUSSION

Protein Structural Changes Induced by Heat Treatment. Regular or plant-based meat shows textural hardening after heat treatment, which is mainly ascribed to the reassembly of protein structures, resulting in the formation of extensive intermolecular interactions and thereby a stronger network.[29,30] Such a hardening approach could provide a simple and low-cost pathway for manufacturing high-strength protein materials. To better understand the mechanism behind this hardening in protein materials, the structural changes were investigated in pure proteins when exposed to heat treatment at pH 7, as shown in Figure 1. IR signal of proteins in the amide I band (1600−1700 cm^{-1}) is particularly sensitive to their secondary structure. To be specific, α-helix, random coil, β-sheet are featured by peaks near 1655, 1643, and 1630 cm^{-1}, respectively, while β-sheet is further distinguished as intra- or intermolecular, possessing peak positions slightly above and below 1630 cm^{-1}, respectively.[31]

Both FTIR and WAXS spectra show that a new structure is formed after heat treatment (as highlighted by the dashed lines in Figure 1). IR spectra show that unheated WPI, SPI, and PPI are characterized by intramolecular β-sheet structures, manifested by peaks close to 1632 cm^{-1} (Figure 1a, black curves). This is in full agreement with previous results[32,33] and is consistent with the resolved protein structures; the major components in WPI and SPI are β-sheet-rich β-lactoglobulin and β-conglycinin, respectively.[34,35] Unheated BSA displays a peak near 1650 cm^{-1}, indicative of α-helix-rich structures (Figure 1a, black curve). Again, this is consistent with the resolved protein structure.[36] Notably, after heat treatment, all the above proteins tend to form a similar structure, the intermolecular β-sheet, contributing to a new peak near 1624 cm^{-1} in the amide I band (Figure 1a), although they possess different initial structures. The analysis of protein secondary structures shows that heated proteins have higher β-sheet content than unheated proteins (Figure S1). The formation of ordered β-sheet structures for heated proteins is also demonstrated by WAXS measurement, indicated by the sharp peak appearing at q = 1.34 $Å^{-1}$, namely, $d = 2\pi/q$ = 4.69 Å (Figures 1b and S2). Typically, 4.69 Å is the distance between adjacent β-strands in the ordered β-sheets.[37,38]

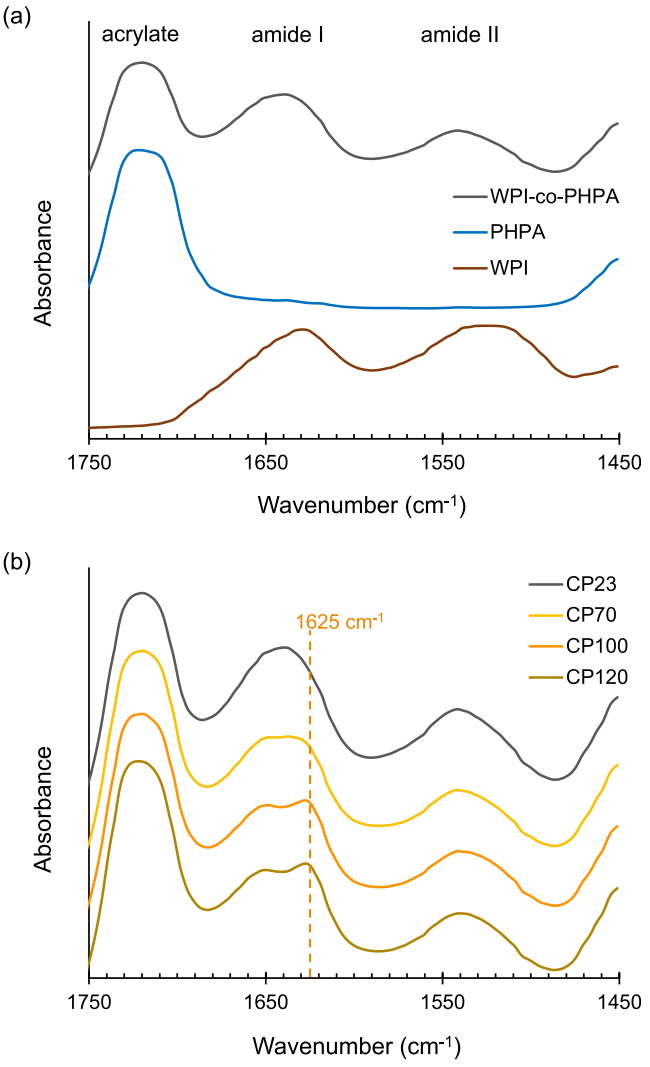

Figure 3. (a) FTIR spectra of WPI-PHPA copolymer, WPI, and PHPA prepared without heat treatment. (b) FTIR spectra of WPI-PHPA copolymer thermosets. CPX refers to the thermoset prepared by incubating the copolymer gel at X °C. The dashed line at ∼1625 cm^{-1} reflects the intermolecular β-sheet structures. The mass ratio of WPI to PHPA is 1/3.

https://doi.org/10.1021/acs.biomac.2c00372
Biomacromolecules 2022, 23, 3286−3295

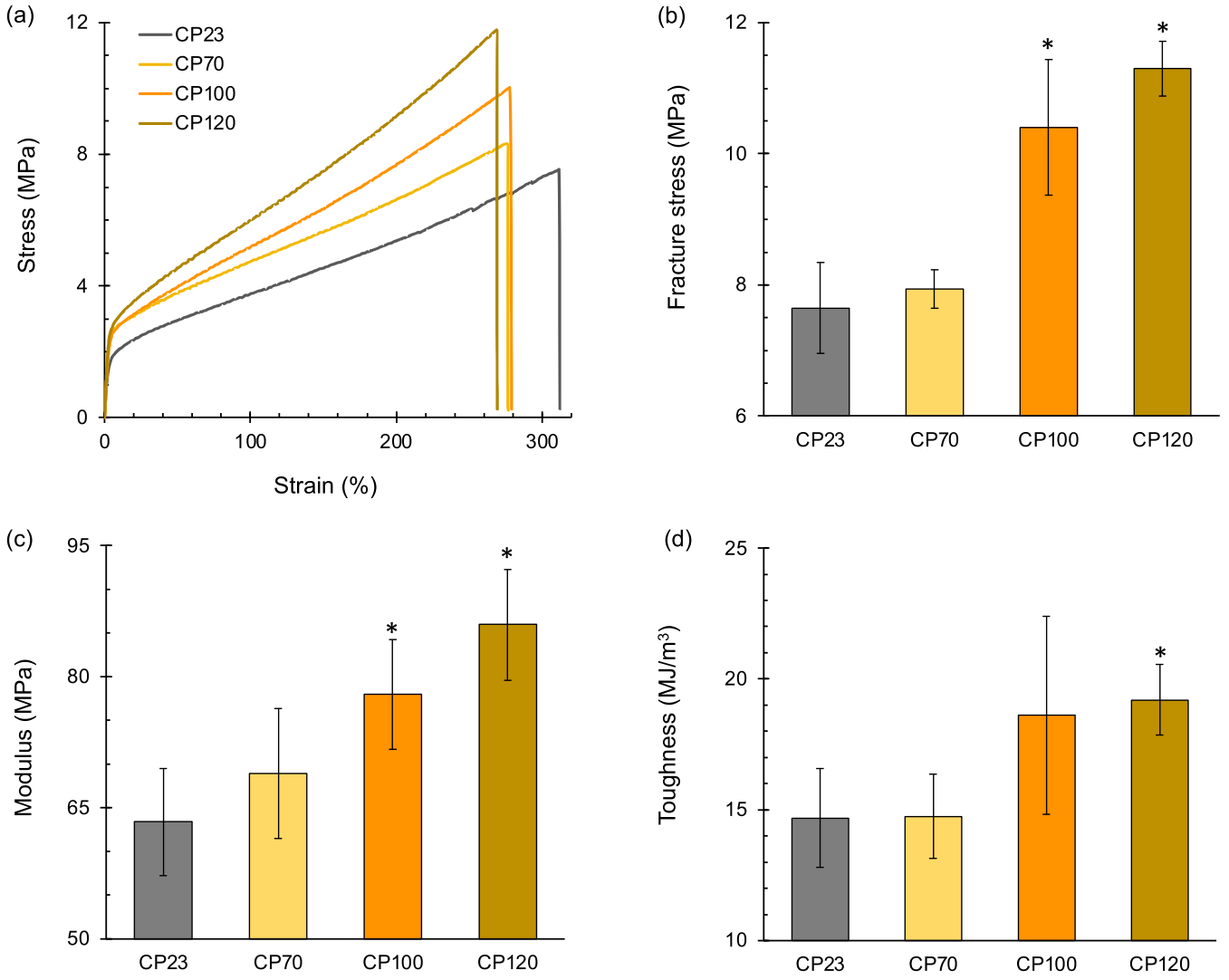

Figure 4. Tensile tests of WPI-PHPA copolymer thermosets. (a) Representative stress−strain curves. (b) Fracture stress. (c) Modulus. (d) Toughness. CPX refers to the thermoset prepared by incubating the copolymer gel at *X* °C. Prior to characterization, these thermosets were equilibrated at 50% relative humidity (RH) and 23 °C for 3 days. The mass ratio of WPI to PHPA is 1/3. Asterisks identify data sets that are statistically ($p < 0.05$) different from the control CP23.

The routine self-assembly of proteins into ordered intermolecular structures can be explained by the well-built protein energy landscape.[39] The native folded and the ordered β-sheet structures are located at local minima of the intramolecular and intermolecular contacts in the protein energy landscape, respectively. Under heat treatment, folded proteins are transferred to partially unfolded states by opening their interior structure, thereby exposing aggregation-prone regions. These unfolded proteins then seek states with lower free energies, where the ordered intermolecular β-sheet structures are likely to form due to possessing the lowest free energies.[39,40] Indeed, self-assembly into amyloid, an ordered intermolecular β-sheet-rich structure, has been demonstrated to be a generic feature of proteins.[38,40] Along with the formation of ordered intermolecular β-sheet structures, proteins may also be entrapped in other intermolecular states such as amorphous aggregates upon heat treatment, as demonstrated by FTIR analysis, showing that β-sheet is not the sole dominant structure in heated samples (Figure S1).

The ordered β-sheets, sometimes described as β-sheet crystals, are the characteristic structure of high-strength proteinaceous materials, including silk and amyloid.[41−43] The β-sheet differences between amyloid and silk include the orientation of β-strands (β-strands are arranged parallel and perpendicular to the fibril long axis in silk and amyloid, respectively), the type of β-sheets (antiparallel and parallel β-sheets are prevalent in silk and amyloid, respectively), and the position of β-sheets (β-crystalline and amorphous regions are arranged like "string-of-beads" in silk, while more like "core−shell cylinder" in amyloid). It needs to be noted that due to the structural complexity of amyloid and silk, in some cases, not all of the above differences are observed.[32] Despite these differences, the β-sheets in both amyloid and silk are highly stacked, leading to high stiffness and modulus.

Fabrication of Protein−Polyacrylate Thermosets. Since the ordered β-sheets are associated with high strength in amyloid and silk, it is valuable to explore the effect of such structures induced by heat treatment on the properties of protein copolymers.

The preparation of protein−polyacrylate copolymer thermosets consists of three steps (Figure 2a): first, proteins are reacted with methacrylic anhydride to yield polymerizable proteins;

https://doi.org/10.1021/acs.biomac.2c00372
Biomacromolecules 2022, 23, 3286−3295

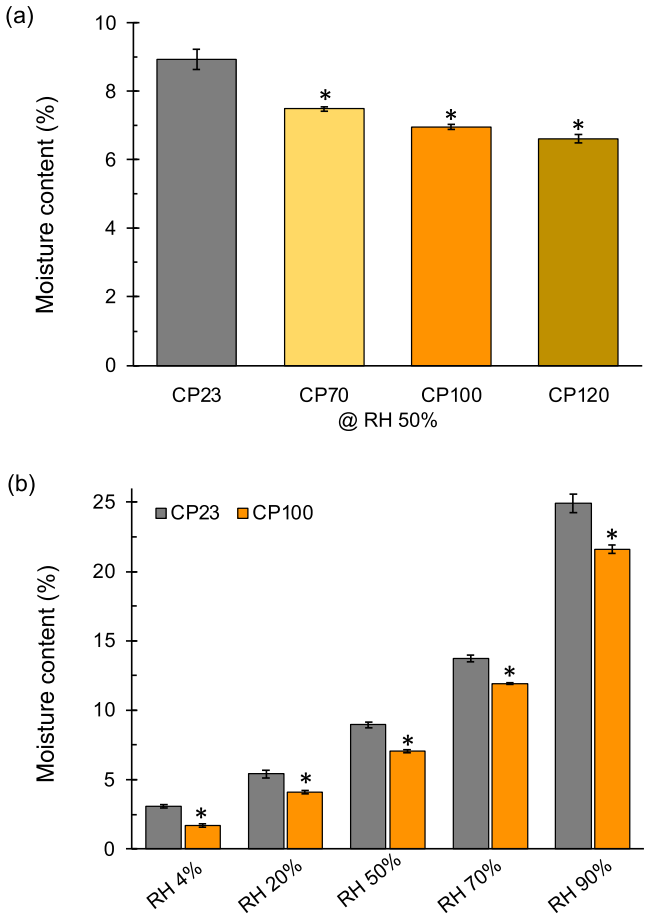

Figure 5. Moisture content of WPI-PHPA copolymer thermosets. (a) Moisture content of thermosets after equilibration at 50% relative humidity (RH). (b) Moisture content of thermosets after equilibration at different humidities. CPX refers to the thermoset prepared by incubating the copolymer gel at X °C. The mass ratio of WPI to PHPA is 1/3. Asterisks identify data sets that are statistically ($p < 0.05$) different from the control CP23 at the corresponding humidity.

second, methacrylated proteins are copolymerized with acrylate monomers to form protein−polyacrylate gel films; and third, the copolymer gel films are incubated at elevated temperatures to trigger the structural unfolding and self-assembly of proteins in hard domains, during which water evaporation leads to the formation of thermoset (CPX). CPX refers to the thermoset prepared by incubating copolymer (CP) gel at X °C. The control thermoset (CP23) was prepared by drying copolymer gel films at room temperature, i.e., without heat treatment. Photographs of copolymers made from whey feedstock are shown in Figure 2b. All thermosets are highly transparent, and those prepared at 70, 100, and 120 °C (CP70, CP100, CP120) exhibit varying degrees of yellowness, which is mainly ascribed to the color of heat-sensitive impurities in the crude protein (Figure S3). However, this color change is not necessarily negative, since commercial polyurethanes are always yellowish.

To focus on elucidating the effect of protein structural changes, the composition and cross-linking density of protein copolymers are fixed in the current study. Specifically, hydroxypropyl acrylate (HPA) is chosen as the soft block, the mass ratio of protein to acrylate is 1:3, and the average degree of methacrylation is ∼3 methacrylate groups per protein molecule. This moderate degree of methacrylation on proteins provides attachment points to the soft block and allows protein structural rearrangements to occur. Previous structural characterization demonstrated that, in this case, protein-PHPA copolymers exhibit protein-rich and PHPA-rich domains (Figure 2a, right), and the thermosets formed after drying are structurally compact rather than porous.[8] The protein-rich domain and low cross-linking density afford the opportunity for molecular rearrangements similar to those in the pure protein system.

Characterization of WPI-PHPA Copolymer Thermosets. Protein structures in copolymers can be detected by FTIR, thanks to the separation of the characteristic bands of protein (amide I and II) and PHPA (acrylate) in the 1750−1450 cm^{-1} region (Figure 3a). Amide I and II bands of CP23 and unheated protein samples are similar, suggesting that protein structures are largely maintained during copolymerization and drying at room temperature. In contrast, copolymers prepared at elevated temperatures (CP70, CP100, CP120) display a new peak near 1625 cm^{-1} in the amide I band (Figure 3b, highlighted by the dashed line), which illustrates that the protein domains of copolymers undergo structural reassembly when exposed to heat treatment, yielding the same intermolecular β-sheet structures as in the pure protein system (Figure 1a). A more pronounced structural transition is observed in copolymers with higher protein content (Figure S4), whereas it is not found for PHPA treated at different temperatures (Figure S5). This data suggests that heating copolymer gels can induce the self-assembly of protein domains, resulting in thermosets with the formation of intermolecular β-sheet structures.

Protein-PHPA copolymers show improved mechanical performance after the formation of intermolecular β-sheet structures. As shown in Figure 4a, thermosets prepared at 70, 100, and 120 °C (CP70, CP100, CP120) have higher stress-at-break without sacrificing much strain-at-break compared to the thermoset CP23. Further increasing incubation temperature impairs the mechanical performance (Figure S6), which may be ascribed to the extensive protein hydrolysis at higher temperatures. Analysis of tensile curves indicates that the fracture stress (Figure 4b), modulus (Figure 4c), and toughness (Figure 4d) are all increased for CP70, CP100, and CP120, and follow the same order as the IR signal intensity at 1625 cm^{-1} in Figure 3b, i.e., a richer intermolecular β-sheet structure corresponds to higher stress, modulus, and toughness. This again demonstrates that the improved mechanical performance is primarily attributed to the formed intermolecular β-sheets in proteins (hard domains of thermosets). CP120 possesses fracture stress of 11.3 ± 0.4 MPa, modulus of 85.9 ± 6.3 MPa, and toughness of 19.2 ± 1.4 MJ/m^3, representing an increase of 48, 36, and 31%, respectively, compared to the thermoset CP23. Importantly, protein copolymers with intermolecular β-sheet structures have mechanical properties similar to those of tough protein materials[9,16,20,44] and are comparable to or exceed those of bio-based polyurethanes.[45−48] Given the economic feasibility[11,12] and mechanical comparability, the developed copolymers could be a valuable alternative to bio-polyurethanes.

The modulus of hybrid materials can be increased by increasing the hard block ratio, but this typically results in considerable sacrifices in strain-at-break as well as stress-at-break and toughness because of the decrease of soft block ratio.[21,49] In contrast, intermolecular structural rearrangement provides a simple strategy to achieve simultaneous increases in modulus, stress, and toughness, with only a small decrease in strain-at-break by reorganizing protein structures in hard domains.

In addition to enhancing the mechanical properties, the formation of intermolecular β-sheets may also alter the

https://doi.org/10.1021/acs.biomac.2c00372
Biomacromolecules 2022, 23, 3286−3295

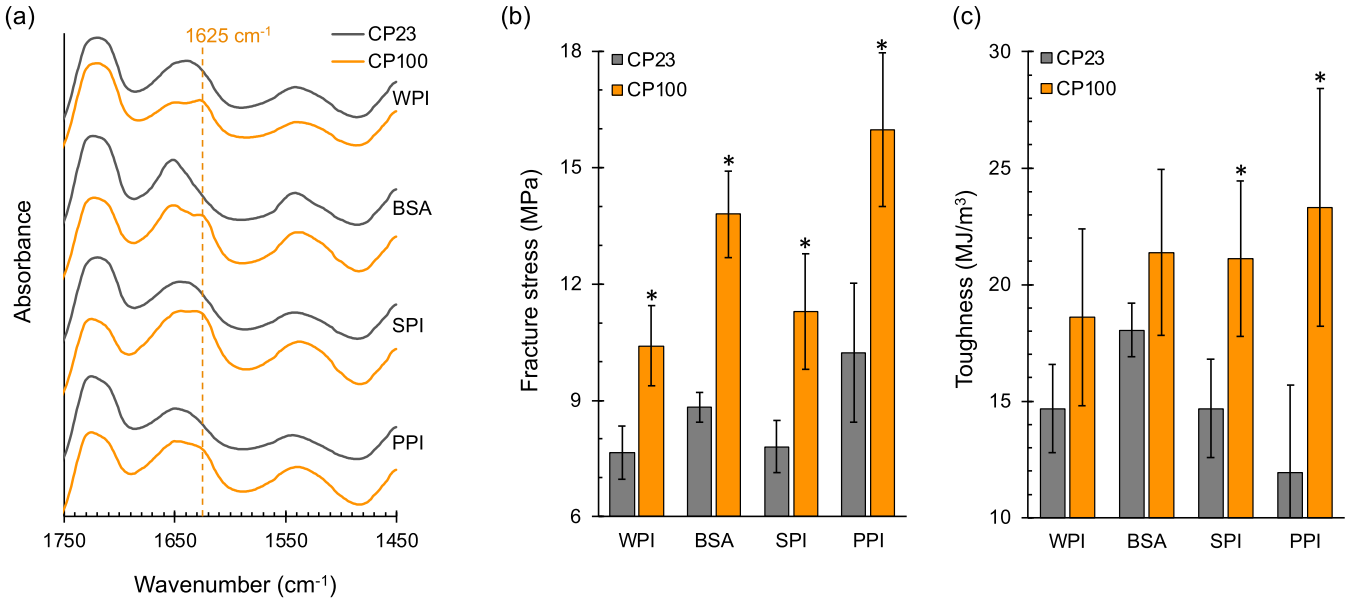

Figure 6. Protein-PHPA copolymer thermosets made from different protein sources. (a) FTIR spectra. (b) Fracture stress. (c) Toughness. CP23 and CP100 refer to thermosets prepared by incubating the copolymer gel at 23 and 100 °C, respectively. The mass ratio of protein to PHPA is 1/3. Asterisks identify data sets that are statistically ($p < 0.05$) different from their control CP23.

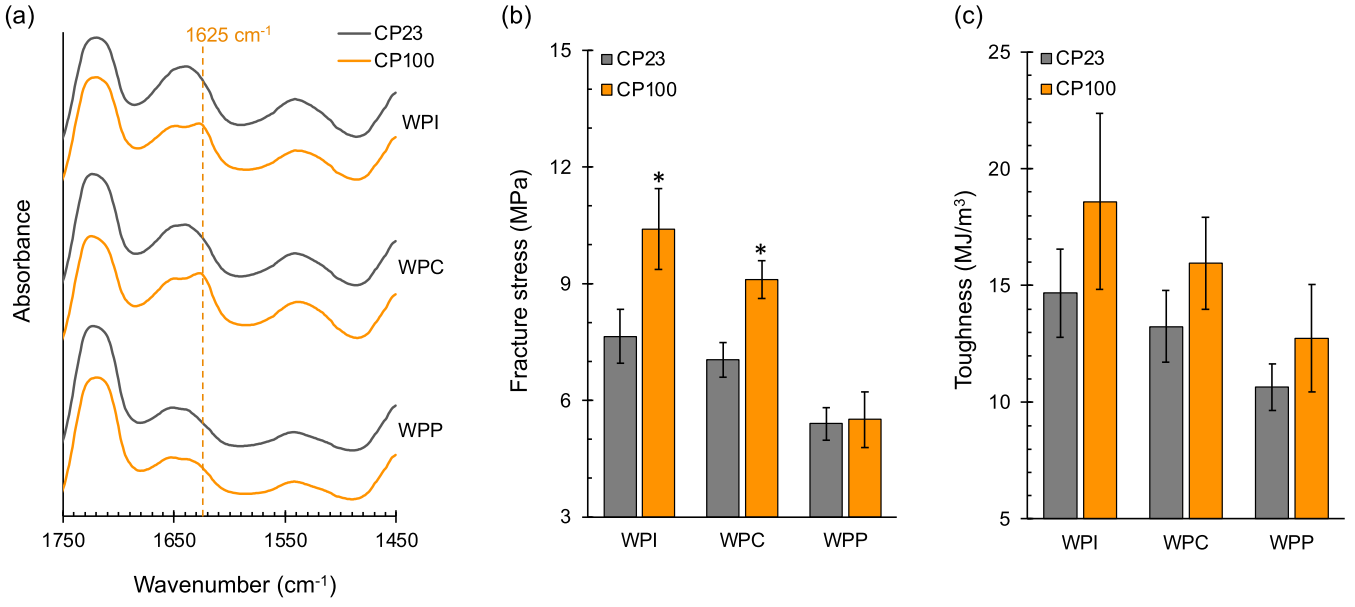

Figure 7. Whey-PHPA copolymer thermosets. (a) FTIR spectra. (b) Fracture stress. (c) Toughness. The protein content of whey protein isolate (WPI), concentrate (WPC), and powder (WPP) is 90.9, 80.6, and 51.2%, respectively (see details in Table S1). CP23 and CP100 refer to thermosets prepared by incubating the copolymer gel at 23 and 100 °C, respectively. The mass ratio of whey to PHPA is 1/3. Asterisks identify data sets that are statistically ($p < 0.05$) different from their control CP23.

hygroscopicity, as the ordered β-sheet structure resembles a crystalline structure that differs from an amorphous structure in terms of the ability to bind water.[50−52] Moisture measurement at relative humidity (RH) = 50% (Figure 5a) shows that copolymer prepared at a higher temperature has a lower moisture content, suggesting the intermolecular β-sheet is capable of reducing the hygroscopicity. CP23 and CP100 were further investigated over an RH range of 4−90% (Figure 5b). It was found that CP100 consistently carries a lower moisture content than CP23 over the investigated humidity range, which again demonstrates that intermolecular β-sheet can lead to the reduction in moisture absorption. Despite the wide availability of natural polymers, including proteins, their application as plastics is also undermined by their hygroscopic nature. These results suggest that the formation of ordered structures is an important strategy for designing less humidity-sensitive materials from natural polymers. Note that the moisture content of protein-PHPA thermosets remains high, which is attributed to the hydrophilic nature of PHPA and can be reduced using hydrophobic soft blocks.[9,10]

Taken together, for the WPI-PHPA system, the thermal treatment of copolymer gels induces structural rearrangement of protein domains, leading to the formation of intermolecular β-sheet structures in the resultant thermosets. The formation of

https://doi.org/10.1021/acs.biomac.2c00372
Biomacromolecules 2022, 23, 3286−3295

this ordered structure further reinforces the hard domains, providing the copolymers with improved strength, toughness, and modulus, as well as reduced hygroscopicity.

Testing the Strengthening−Toughening Mechanism in Different Protein Systems. The intermolecular β-sheets can be generated not only from WPI but also from other proteins (Figure 1). To verify whether the main findings in the WPI system are also present in other protein systems, copolymers composed of other proteins and PHPA were fabricated and characterized.

Similar to the CP100 made from WPI, CP100s made from BSA, SPI, and PPI also show a new peak near 1625 cm^{-1} in the amide I band (Figure 6a), indicating that protein domains of these copolymers also undergo structural self-assembly upon heat treatment, forming intermolecular β-sheet structures. Analysis of tensile tests shows that CP100 has higher fracture stress and toughness compared to CP23, observed in all protein systems (Figure 6b,c). This again demonstrates that the formation of intermolecular β-sheet structures in protein domains can be used for improving strength and toughness and suggests that this strengthening−toughening mechanism is general for many protein feedstocks. The magnitude of the improvements varies from protein to protein, which may be induced by the sequence-dependent stability of intermolecular β-sheet structures. On the other hand, the formation of intermolecular β-sheet structures can give rise to a decrease in moisture absorption observed in all investigated protein systems (Figure S7).

Next, the effect of the protein purity on copolymer formation and mechanical properties was investigated. Two commercially available whey products with lower protein content were examined: whey protein concentrate (WPC, 80.6% protein content) and whey protein powder (WPP, 51.2% protein content) (Table S1). Similar to WPI, transparent thermosets were successfully developed from WPC and WPP (Figure S8). This illustrates the formation of thermosets with lower purity feedstocks and signifies the great promise of this method in practical applications. The high transparency also suggests that the formed thermosets are in copolymer form, as the protein-PHPA blends are observed to be opaque.[8] Tensile tests showed that the mechanical properties of WPC-PHPA and WPP-PHPA are slightly weaker than WPI-PHPA (Figure 7b,c). This can be understood by the fact that although three types of whey-PHPA thermosets have the same whey/PHPA mass ratio, the WPC-PHPA and WPP-PHPA thermosets contain less protein due to the lower protein content in their initial whey products (Table S1). Furthermore, it was found that heat treatment resulted in the strengthening of WPC copolymers, which is insignificant in WPP, indicating that protein purity, although not affecting copolymer formation, can influence protein reassembly. Indeed, FTIR revealed the formation of intermolecular β-sheet in WPI and WPC copolymers after thermal treatment but not in WPP copolymer (Figure 7a).

The strengthening−toughening effect of intermolecular β-sheets is also demonstrated in copolymers synthesized using the preformed intermolecular β-sheet-rich protein (referred to as β-sheet WPI). In these copolymers, the intermolecular β-sheets are generated and purified prior to copolymerization with acylate monomers. Tensile tests indicate that the modulus, strength, and toughness of copolymers made from β-sheet WPI are 6, 2, and 2 times those of copolymers made from WPI monomer (Figure S9). The more significant improvement than in Figure 4 can be attributed to the more abundant intermolecular β-sheet structures for β-sheet WPI (Figure S10). However, β-sheet WPI is not favorable for the preparation of copolymers with high protein content because increasing its concentration causes solution viscosities high enough to impede mixing.

The copolymers developed in this study are, in principle, not fully biodegradable because they contain polyacrylate segments. Despite their nonbiodegradability, these protein-based thermosets have notable merits over synthetic ones in terms of the reduced dependence on fossil resources and the contribution to carbon sequestration. Their carbon sequestration is the result of atmospheric carbon dioxide required for protein biosynthesis/formation, leading to atmospheric carbon being stored throughout the use of the thermosets.

CONCLUSIONS

In summary, protein copolymers can be efficiently synthesized from a broad range of protein feedstocks by protein methacrylation followed by copolymerization with acrylate monomers. A simple heat treatment of these protein copolymer gels can result in molded thermosets with improved mechanical properties. This arises from the thermally induced structural rearrangements of proteins in hard domains forming ordered intermolecular β-sheets, which reinforce the hard domains and lead to increased modulus, strength, and toughness. The strengthening−toughening mechanism of intermolecular β-sheet structures was also demonstrated using different protein sources as well as the pre-prepared intermolecular β-sheeted proteins. In addition, the intermolecular β-sheet structures can reduce the hygroscopicity of the material, analogous to crystalline structures. Therefore, this study not only provides a simple yet effective strategy for expanding the application of protein feedstocks but also reveals the significance of protein molecular structures in designing high-performance materials.

ASSOCIATED CONTENT

Supporting Information

The Supporting Information is available free of charge at https://pubs.acs.org/doi/10.1021/acs.biomac.2c00372.

Table S1 and Figures S1−S12 (PDF)

AUTHOR INFORMATION

Corresponding Author

Bradley D. Olsen − *Department of Chemical Engineering, Massachusetts Institute of Technology, Cambridge, Massachusetts 02139, United States;* orcid.org/0000-0002-7272-7140; Email: bdolsen@mit.edu

Author

Yiping Cao − *Department of Chemical Engineering, Massachusetts Institute of Technology, Cambridge, Massachusetts 02139, United States;* orcid.org/0000-0002-7039-5445

Complete contact information is available at: https://pubs.acs.org/10.1021/acs.biomac.2c00372

Notes

The authors declare no competing financial interest.

ACKNOWLEDGMENTS

This work was supported by the Abdul Latif Jameel Water and Food Systems Lab (J-WAFS) at MIT. The authors thank the

Department of Chemistry Instrumentation Facility for the use of FTIR equipment and the Materials Research Science and Engineering Center for the use of WAXS equipment. Y.C. acknowledges the Swiss National Science Foundation (SNSF) for financial support.

REFERENCES

(1) Mekonnen, T.; Mussone, P.; Khalil, H.; Bressler, D. Progress in Bio-Based Plastics and Plasticizing Modifications. *J. Mater. Chem. A* **2013**, *1*, 13379−13398.
(2) Emadian, S. M.; Onay, T. T.; Demirel, B. Biodegradation of Bioplastics in Natural Environments. *Waste Manage.* **2017**, *59*, 526−536.
(3) Xie, F.; Pollet, E.; Halley, P. J.; Avérous, L. Starch-Based Nano-Biocomposites. *Prog. Polym. Sci.* **2013**, *38*, 1590−1628.
(4) Williams, C. K.; Hillmyer, M. A. Polymers from Renewable Resources: A Perspective for a Special Issue of Polymer Reviews. *Polym. Rev.* **2008**, *48*, 1−10.
(5) Szycher, M. *Szycher's Handbook of Polyurethanes*,, 2nd ed.; CRC Press: Boca Raton, FL, 2012; pp 37−86.
(6) Meier, M. A. R. Plant-Oil-Based Polyamides and Polyurethanes: Toward Sustainable Nitrogen-Containing Thermoplastic Materials. *Macromol. Rapid Commun.* **2019**, *40*, No. 1800524.
(7) Firdaus, M.; Meier, M. A. R. Renewable Polyamides and Polyurethanes Derived from Limonene. *Green Chem.* **2013**, *15*, 370−380.
(8) Chan, W. Y.; Bochenski, T.; Schmidt, J. E.; Olsen, B. D. Peptide Domains as Reinforcement in Protein-Based Elastomers. *ACS Sustainable Chem. Eng.* **2017**, *5*, 8568−8578.
(9) Chan, W. Y.; King, E. J.; Olsen, B. D. Hydrophobic and Bulk Polymerizable Protein-Based Elastomers Compatibilized with Surfactants. *ACS Sustainable Chem. Eng.* **2019**, *7*, 9103−9111.
(10) Andersen, E.; Wui, A.; Chan, Y.; Sureka, H. V.; Olsen, B. D. Tuning Compatibility and Water Uptake by Protein Charge Modification in Melt-Polymerizable Protein-Based Thermosets. *Mater. Adv.* **2022**, *3*, 2158−2169.
(11) Bochenski, T.; Chan, W. Y.; Olsen, B. D.; Schmidt, J. E. Techno-Economic Analysis for the Production of Novel Bio-Derived Elastomers with Modified Algal Proteins as a Reinforcing Agent. *Biorefinery* **2019**, 639−654.
(12) Chalermthai, B.; Ashraf, M. T.; Bastidas-Oyanedel, J. R.; Olsen, B. D.; Schmidt, J. E.; Taher, H. Techno-Economic Assessment of Whey Protein-Based Plastic Production from a Co-Polymerization Process. *Polymers* **2020**, *12*, No. 847.
(13) Poore, J.; Nemecek, T. Reducing Food's Environmental Impacts through Producers and Consumers. *Science* **2018**, *360*, 987−992.
(14) Verbeek, C. J. R.; Van Den Berg, L. E. Extrusion Processing and Properties of Protein-Based Thermoplastics. *Macromol. Mater. Eng.* **2010**, *295*, 10−21.
(15) Shaw, N. B.; Monahan, F. J.; O'Riordan, E. D.; O'Sullivan, M. Physical Properties of WPI Films Plasticized with Glycerol, Xylitol, or Sorbitol. *J. Food Sci.* **2002**, *67*, 164−167.
(16) Ye, X.; Junel, K.; Gällstedt, M.; Langton, M.; Wei, X. F.; Lendel, C.; Hedenqvist, M. S. Protein/Protein Nanocomposite Based on Whey Protein Nanofibrils in a Whey Protein Matrix. *ACS Sustainable Chem. Eng.* **2018**, *6*, 5462−5469.
(17) Perriman, A. W.; Cölfen, H.; Hughes, R. W.; Barrie, C. L.; Mann, S. Solvent-Free Protein Liquids and Liquid Crystals. *Angew. Chem., Int. Ed.* **2009**, *48*, 6242−6246.
(18) Perriman, A. W.; Mann, S. Liquid Proteins−A New Frontier for Biomolecule-Based Nanoscience. *ACS Nano* **2011**, *5*, 6085−6091.
(19) Jong, L. Characterization of Soy Protein/Styrene−Butadiene Rubber Composites. *Composites, Part A* **2005**, *36*, 675−682.
(20) Peydayesh, M.; Bagnani, M.; Mezzenga, R. Sustainable Bioplastics from Amyloid Fibril-Biodegradable Polymer Blends. *ACS Sustainable Chem. Eng.* **2021**, *9*, 11916−11926.
(21) Hamad, K.; Kaseem, M.; Ayyoob, M.; Joo, J.; Deri, F. Polylactic Acid Blends: The Future of Green, Light and Tough. *Prog. Polym. Sci.* **2018**, *85*, 83−127.
(22) Porter, D.; Vollrath, F. Silk as a Biomimetic Ideal for Structural Polymers. *Adv. Mater.* **2009**, *21*, 487−492.
(23) Li, J.; Zhu, Y.; Yu, H.; Dai, B.; Jun, Y. S.; Zhang, F. Microbially Synthesized Polymeric Amyloid Fiber Promotes β-Nanocrystal Formation and Displays Gigapascal Tensile Strength. *ACS Nano* **2021**, *15*, 11843−11853.
(24) Rathore, O.; Sogah, D. Y. Nanostructure Formation through β-Sheet Self-Assembly in Silk-Based Materials. *Macromolecules* **2001**, *34*, 1477−1486.
(25) Rathore, O.; Sogah, D. Y. Self-Assembly of β-Sheets into Nanostructures by Poly(Alanine) Segments Incorporated in Multiblock Copolymers Inspired by Spider Silk. *J. Am. Chem. Soc.* **2001**, *123*, 5231−5239.
(26) Andersson, L.; Blomberg, L.; Flegel, M.; Lepsa, L.; Nilsson, B.; Verlander, M. Large-Scale Synthesis of Peptides. *Pept. Sci.* **2000**, *55*, 227−250.
(27) Mollea, C.; Marmo, L.; Bosco, F. Valorisation of Cheese Whey, A By-Product from the Dairy Industry. In *Food Industry*, IntechOpen, 2013.
(28) Kumar, R.; Choudhary, V.; Mishra, S.; Varma, I. K.; Mattiason, B. Adhesives and Plastics Based on Soy Protein Products. *Ind. Crops Prod.* **2002**, *16*, 155−172.
(29) Bertola, N. C.; Bevilacqua, A. E.; Zaritzky, N. E. Heat Treatment Effect on Texture Changes and Thermal Denaturation of Proteins in Beef Muscle. *J. Food Process. Preserv.* **1994**, *18*, 31−46.
(30) Palka, K.; Daun, H. Changes in Texture, Cooking Losses, and Myofibrillar Structure of Bovine M. Semitendinosus during Heating. *Meat Sci.* **1999**, *51*, 237−243.
(31) Zandomeneghi, G.; Krebs, M. R. H.; McCammon, M. G.; Fändrich, M. FTIR Reveals Structural Differences between Native β-Sheet Proteins and Amyloid Fibrils. *Protein Sci.* **2009**, *13*, 3314−3321.
(32) Cao, Y.; Adamcik, J.; Diener, M.; Kumita, J. R.; Mezzenga, R. Different Folding States from the Same Protein Sequence Determine Reversible vs Irreversible Amyloid Fate. *J. Am. Chem. Soc.* **2021**, *143*, 11473−11481.
(33) Kamada, A.; Rodriguez-Garcia, M.; Ruggeri, F. S.; Shen, Y.; Levin, A.; Knowles, T. P. J. Controlled Self-Assembly of Plant Proteins into High-Performance Multifunctional Nanostructured Films. *Nat. Commun.* **2021**, *12*, No. 3529.
(34) Qin, B. Y.; Jameson, G. B.; Bewley, M. C.; Baker, E. N.; Creamer, L. K. Functional Implications of Structural Differences between Variants A and B of Bovine β-Lactoglobulin. *Protein Sci.* **2008**, *8*, 75−83.
(35) Maruyama, N.; Adachi, M.; Takahashi, K.; Yagasaki, K.; Kohno, M.; Takenaka, Y.; Okuda, E.; Nakagawa, S.; Mikami, B.; Utsumi, S. Crystal Structures of Recombinant and Native Soybean β-Conglycinin β Homotrimers. *Eur. J. Biochem.* **2001**, *268*, 3595−3604.
(36) Bujacz, A. Structures of Bovine, Equine and Leporine Serum Albumin. *Acta Crystallogr., Sect. D* **2012**, *68*, 1278−1289.
(37) Eisenberg, D. S.; Sawaya, M. R. Structural Studies of Amyloid Proteins at the Molecular Level. *Annu. Rev. Biochem.* **2017**, *86*, 69−95.
(38) Ke, P. C.; Zhou, R.; Serpell, L. C.; Riek, R.; Knowles, T. P. J.; Lashuel, H. A.; Gazit, E.; Hamley, I. W.; Davis, T. P.; Fändrich, M.; Otzen, D. E.; Chapman, M. R.; Dobson, C. M.; Eisenberg, D. S.; Mezzenga, R. Half a Century of Amyloids: Past, Present and Future. *Chem. Soc. Rev.* **2020**, *49*, 5473−5509.
(39) Adamcik, J.; Mezzenga, R. Amyloid Polymorphism in the Protein Folding and Aggregation Energy Landscape. *Angew. Chem., Int. Ed.* **2018**, *57*, 8370−8382.
(40) Cao, Y.; Mezzenga, R. Food Protein Amyloid Fibrils: Origin, Structure, Formation, Characterization, Applications and Health Implications. *Adv. Colloid Interface Sci.* **2019**, *269*, 334−356.
(41) Ling, S.; Kaplan, D. L.; Buehler, M. J. Nanofibrils in Nature and Materials Engineering. *Nat. Rev. Mater.* **2018**, *3*, 18016.
(42) Ling, S.; Li, C.; Adamcik, J.; Shao, Z.; Chen, X.; Mezzenga, R. Modulating Materials by Orthogonally Oriented β-Strands: Compo-

https://doi.org/10.1021/acs.biomac.2c00372
Biomacromolecules 2022, 23, 3286−3295

sites of Amyloid and Silk Fibroin Fibrils. *Adv. Mater.* **2014**, *26*, 4569−4574.
(43) Adamcik, J.; Ruggeri, F. S.; Berryman, J. T.; Zhang, A.; Knowles, T. P. J.; Mezzenga, R. Evolution of Conformation, Nanomechanics, and Infrared Nanospectroscopy of Single Amyloid Fibrils Converting into Microcrystals. *Adv. Sci.* **2021**, *8*, No. 2002182.
(44) Duraj-Thatte, A. M.; Manjula-Basavanna, A.; Courchesne, N. M. D.; Cannici, G. I.; Sánchez-Ferrer, A.; Frank, B. P.; van't Hag, L.; Cotts, S. K.; Fairbrother, D. H.; Mezzenga, R.; Joshi, N. S. Water-Processable, Biodegradable and Coatable Aquaplastic from Engineered Biofilms. *Nat. Chem. Biol.* **2021**, *17*, 732−738.
(45) Poussard, L.; Mariage, J.; Grignard, B.; Detrembleur, C.; Jéroîme, C.; Calberg, C.; Heinrichs, B.; De Winter, J.; Gerbaux, P.; Raquez, J. M.; Bonnaud, L.; Dubois, P. Non-Isocyanate Polyurethanes from Carbonated Soybean Oil Using Monomeric or Oligomeric Diamines To Achieve Thermosets or Thermoplastics. *Macromolecules* **2016**, *49*, 2162−2171.
(46) Kim, H.; Cha, I.; Yoon, Y.; Cha, B. J.; Yang, J.; Kim, Y. D.; Song, C. Facile Mechanochemical Synthesis of Malleable Biomass-Derived Network Polyurethanes and Their Shape-Memory Applications. *ACS Sustainable Chem. Eng.* **2021**, *9*, 6952−6961.
(47) Chen, H.; Chauhan, P.; Yan, N. "Barking" up the Right Tree: Biorefinery from Waste Stream to Cyclic Carbonate with Immobilization of CO2 for Non-Isocyanate Polyurethanes. *Green Chem.* **2020**, *22*, 6874−6888.
(48) Sternberg, J.; Pilla, S. Materials for the Biorefinery: High Bio-Content, Shape Memory Kraft Lignin-Derived Non-Isocyanate Polyurethane Foams Using a Non-Toxic Protocol. *Green Chem.* **2020**, *22*, 6922−6935.
(49) Ritchie, R. O. The Conflicts between Strength and Toughness. *Nat. Mater.* **2011**, *10*, 817−822.
(50) Bronlund, J.; Paterson, T. Moisture Sorption Isotherms for Crystalline, Amorphous and Predominantly Crystalline Lactose Powders. *Int. Dairy J.* **2004**, *14*, 247−254.
(51) Mihranyan, A.; Llagostera, A. P.; Karmhag, R.; Strømme, M.; Ek, R. Moisture Sorption by Cellulose Powders of Varying Crystallinity. *Int. J. Pharm.* **2004**, *269*, 433−442.
(52) Hofstetter, K.; Hinterstoisser, B.; Salmén, L. Moisture Uptake in Native Cellulose − the Roles of Different Hydrogen Bonds: A Dynamic FT-IR Study Using Deuterium Exchange. *Cellulose* **2006**, *13*, 131−145.

https://doi.org/10.1021/acs.biomac.2c00372
Biomacromolecules 2022, 23, 3286−3295